Formation of Fe-rich intermetallic compounds and their effect on the tensile properties of squeeze-cast Al–Cu alloys

Wei-wen Zhang
Department of Material Forming and Control Engineering, School of Mechanical and Automotive Engineering, South China University of Technology, Guangzhou 510640, People's Republic of China

Bo Lin[a)]
Department of Material Forming and Control Engineering, School of Mechanical and Automotive Engineering, South China University of Technology, Guangzhou 510640, People's Republic of China; and Department of Material Forming and Control Engineering, School of Mechanical Engineering, Gui Zhou University, Guiyang 550025, People's Republic of China

Zhi Luo, Yu-liang Zhao, and Yuan-yuan Li
Department of Material Forming and Control Engineering, School of Mechanical and Automotive Engineering, South China University of Technology, Guangzhou 510640, People's Republic of China

(Received 6 April 2015; accepted 23 June 2015)

The development of high performance Al–Cu based alloys generally depends on the strict control of the Fe content. However, with the increasing use of recycled aluminum alloys, it is necessary to increase the tolerance for the Fe content in Al–Cu cast alloys for the purpose of low cost, energy saving, and environment protection. In this study, the formation of Fe-rich intermetallics and their effect on the tensile properties of squeeze-cast Al–5.0 wt% Cu–0.6 wt% Mn alloys with an Fe content of up to 1.5 wt% have been investigated. The full formation sequence of squeeze-cast Al–5.0 wt% Cu–0.6 wt% Mn alloys with different Fe contents has been established. The results were also compared with the corresponding results obtained for Al–5.0Cu–0.6Mn alloys prepared by gravity die casting. It is found that the Fe-rich intermetallic compounds mainly consist of α-Fe and β-Fe in alloys with a low Fe content, changing into Al_6(FeMn) and Al_3(FeMn) for alloys with a high Fe content. The applied pressure promotes the formation of the Fe-rich intermetallics α-Fe/Al_6(FeMn) and prevents the precipitation of needle-like β-Fe/Al_3(FeMn). The elongation of the alloys gradually decreases with the Fe content, and a maximum value for both the ultimate mechanical strength and the yield strength was found for the alloys with 0.5 wt% Fe. The tensile properties of alloys with a different Fe content significantly increased as the applied pressure was increased from 0 to 75 MPa, especially the elongation.

I. INTRODUCTION

With increasing use of recycled aluminum alloys, the control of Fe impurities has become a great challenge for the low cost aluminum industry. Fe impurities are inevitable and considered to be most detrimental to the tensile properties. To reduce the detrimental effect of Fe impurities on aluminum alloys, the formation of Fe-rich intermetallics and their effect on the tensile properties have been widely investigated. However, most of these studies focused on Al–Si alloys.[1–4] Only a few studies have been reported focusing on the formation of Fe-rich intermetallics in Al–Cu cast alloys. The needle-like β-Fe (Al_7Cu_2Fe) phase is the most frequently observed Fe-rich intermetallic compound found in A206 Al–Cu alloys with a low Fe content, as reported by Backerud et al.,[5] Talamantes-Silva et al.,[6] and Tseng et al.[7] Mn and Si were added to the alloys to transform the Fe-rich intermetallics from the needle-like β-Fe to the less detrimental α-Fe phase.[8–12]

Recently, Liu et al. reported on the formation of Fe-rich intermetallics in A206 alloys with 0.5% Fe[13–15](all compositions quoted in this work are in weight percent unless indicated otherwise). They found that the needle-like Al_3(FeMn), Al_mFe and α-Fe all represent potential dominant Fe-rich intermetallic phases of the solidified microstructure in Al–Cu alloys, depending on the Fe, Mn and Si content, and the applied cooling rate. Liu et al. also studied the effect of Fe-rich intermetallics on the tensile properties of A206 alloys containing 0.5% Fe,[16] and reported that the Chinese-script Fe-rich intermetallics are less detrimental to the tensile properties than the needle-like Fe-rich phase (β-Fe), and that the required ductility (>7%) and mechanical strength can be reached under T4 condition. Therefore, it is possible to design recycled Al–Cu cast alloys with a high Fe content.

Squeeze casting is an efficient method to develop high performance and low cost aluminum alloys with higher

Contributing Editor: Jürgen Eckert
[a)]Address all correspondence to this author.
e-mail: linbo1234@126.com
DOI: 10.1557/jmr.2015.215

Fe contents.[17–19] However, only a few studies on the formation of Fe-rich intermetallic compounds in squeeze-cast Al–Cu alloys and their effect on the tensile properties have been reported. Therefore, in this study, the formation of Fe-rich intermetallics and their effect on the tensile properties of squeeze-cast Al–5.0Cu–0.6Mn alloys with different Fe contents were investigated. The results are expected to be helpful for the development of high performance cast Al–Cu alloys with high Fe content.

II. MATERIAL AND METHODS

Commercially pure Al (99.5%), Al–50% Cu, Al–10% Mn, and Al–5% Fe master alloys were used to prepare the experimental alloys, and their chemical composition was analyzed using an optical emission spectrometer. The composition of the experimental alloys is listed in Table I. The raw materials were melted at 1053 K in a clay-graphite crucible using an electric resistance furnace. About 10 kg of the melts were degassed using 0.5% C_2Cl_6 to minimize the hydrogen content. Next, the melt was poured into a cylindrical die under different applied pressures in the range from 0 and 75 MPa. The die temperature was set to approximately 250 °C, and the pouring temperature was set to 710 °C before squeeze casting. Finally, cylindrical samples with a height of 65 mm and a diameter of 68 mm were obtained.

Samples for the mechanical tests with a diameter of 10 mm and a height of 65 mm were produced using a line-cutting machine. The mechanical tests were performed using a SANS CMT5105 standard testing machine. The values reported here were averaged over three samples. Samples for the metallographic observation were cut from the gage length part of selected mechanical specimens and then etched in a 0.5% HF solution for 30 s. A Leica optical microscope equipped with the image analysis software Leica materials workstation V3.6.1 was used to quantitatively analyze the Fe-rich intermetallics. To obtain statistically significant data, approximately 50 different regions around the center of the etched specimen were investigated at a magnification factor of 500. The average phase composition and the fracture surfaces of the mechanical specimens were analyzed using a Nova Nano SEM 430 scanning electron microscope (SEM, Hillsboro, OR), equipped with an energy-dispersive x-ray analyzer. To further reveal the 3D morphology of the intermetallics, some samples were deep-etched to preferentially remove the matrix phase. Deep etching was carried out on alloy samples that were mounted and polished to 1 μm diamond and then were immersed face down in a gently stirred solution of iodine in methanol (10 g in 100 mL) at room temperature for 4–5 h.[20] The samples were then gently rinsed with methanol and dried in air prior to the SEM investigations. A differential scanning calorimetry (DSC; NETZSCH STA449 C, Bavaria, Germany) analysis using a heating rate of 10 K min^{-1} was performed to study the solidification reactions and temperatures. An x-ray diffraction (XRD) analysis was performed (Bruker D8 ADVANCE, Karlsruhe, Germany) to study the phase evolution. To increase the percentage of the Fe-rich intermetallics, powder samples of the experimental alloys were also bathed in a solution of iodine in methanol (10 g in 100 mL) for approximately 24 h and then investigated by XRD. In addition, interrupted water quenching at different temperatures was also adopted to identify the Fe-rich intermetallics. A special mold with fast opened and closed bottom plate was used to solidify the experimental alloys, then the casting was quenched into ice water less than 1 s. During the cooling, a K-type thermocouple was positioned in the center of the crucible to measure the temperature.

TABLE I. Chemical compositions of the experimental alloys (wt%).

Alloys	Cu	Mn	Fe	Si	Al
Al–5.0Cu–0.6Mn–0.1Fe(Fe01)	5.00	0.60	0.12	0.08	Balance
Al–5.0Cu–0.6Mn–0.5Fe(Fe05)	4.92	0.59	0.46	0.08	Balance
Al–5.0Cu–0.6Mn–0.7Fe(Fe07)	5.20	0.65	0.74	0.06	Balance
Al–5.0Cu–0.6Mn–1.0Fe(Fe10)	5.15	0.61	1.05	0.07	Balance
Al–5.0Cu–0.6Mn–1.5Fe(Fe15)	5.44	0.60	1.51	0.08	Balance

III. RESULTS

A. Formation of Fe-rich intermetallics in Al–5.0Cu–0.6Mn alloys

The Fe-rich intermetallics found in the experimental alloys with different Fe contents are shown in Fig. 1. Four different Fe-rich intermetallics were found in the Al–5.0Cu–0.5Fe alloys, including α-Fe [$Al_{15}(FeMn)_3(CuSi)_2$] and $Al_6(FeMn)$, the needle-like $Al_3(FeMn)$, and β-Fe [$Al_7Cu_2(FeMn)$]. The average composition of the Fe-rich intermetallics as obtained by a scanning electron microscope equipped with energy dispersive x-ray spectrometry (SEM-EDS) analysis is compared in Table II. The α-Fe phase contains a small amount of Si, while the β-Fe phase contains a high amount of Cu.

The evolution of Fe-rich intermetallics with increasing Fe content was investigated by XRD analysis. The XRD pattern obtained for Fe10 alloys without deep etching is shown in Fig. 2(a). Only the α (Al) and Al_2Cu phases were found in the Fe10 samples, and diffraction peaks associated with the Fe-rich intermetallics are barely visible due to the low percentage of Fe-rich intermetallics within the samples. To remove the matrix phase and increase the percentage of the Fe-rich intermetallics, some powder samples were deep etched in a solution of iodine in methanol (10 g in 100 mL) for approximately 24 h. The resulting XRD patterns for deep etched samples are shown in Figs. 2(b)–2(d). We found that the Fe-rich intermetallics consist of α-Fe for Al–5.0Cu–0.6Mn alloys with a low Fe content, and they change into $Al_6(FeMn)$ and $Al_3(FeMn)$ for alloys with a high Fe content.

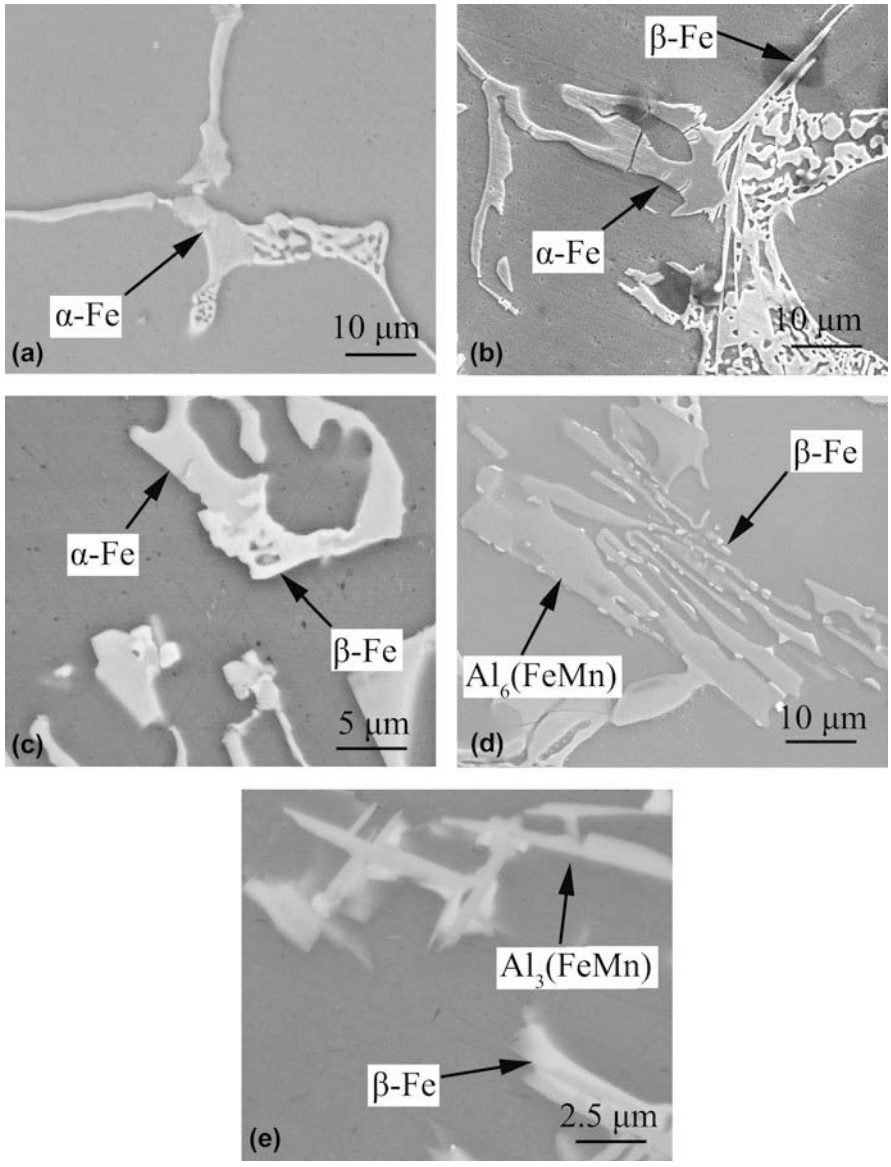

FIG. 1. SEM morphology of Fe-rich intermetallics in alloys with different Fe contents: (a) 0.1%; (b) 0.5%; (c) 0.7%; (d) 1.0%; (e) 1.5%.

B. Formation of Fe-rich intermetallics in gravity die cast alloys

Figure 3 shows the DSC heating curves obtained for the gravity die cast alloys. Three distinct peaks can be identified. To investigate the formation of the Fe-rich intermetallics in detail, an interrupted water quenching technique was used to observe the Fe-rich intermetallics formed at different temperatures. The microstructure of gravity die cast alloys water quenched at 620, 600, and 570 °C, respectively, is revealed in Fig. 4. As shown in Fig. 4(a), the Fe-rich intermetallics consist of Al_6(FeMn) for the samples water quenched at 620 °C and change into α-Fe [Fig. 4(b)] or β-Fe. Similar results were observed for the Fe07 alloy. When the Fe content was increased to 1.0%, the Fe-rich intermetallics consist of Al_6(FeMn) and Al_3(FeMn) for the samples water quenched at 620 °C, with the Al_3(FeMn) partly changing into Al_6(FeMn), effectively resulting in the decrease of the Al_3(FeMn) content in samples water quenched at 570 °C.

C. Effect of the applied pressure on the formation of Fe-rich intermetallics

The DSC heating curves obtained for the alloys squeeze-cast at 75 MPa are shown in Fig. 5. Similar to the results obtained for the gravity die cast alloys, three peaks were observed for the squeeze-cast alloys. To investigate the effect of the applied pressure on the formation of the Fe-rich intermetallics, the samples squeeze-cast at 75 MPa were water quenched at 620 °C, as shown in Fig. 6. Compared to the microstructure of water

quenched gravity die cast alloys, the size of the Fe-rich intermetallic phases is smaller and the amount of Al_3(FeMn) is obviously lower in the squeeze-cast alloys [Fig. 6(c)].

The volume percent of the Fe-rich intermetallic phases in alloys with a different Fe content and for different applied pressures is shown in Fig. 7. The volume percent of the Fe-rich intermetallics obviously increases with the Fe content, while the applied pressure decreases the volume percent of needle-like Fe-rich intermetallics obviously. When the applied pressures increase from 0 to 75 MPa, the volume percent of needle-like Al_3(FeMn) in Fe10 alloys decreases from 3.5 to 0.6%.

TABLE II. Average chemical composition of Fe-rich intermetallics (at %).

Source	Phase	Al	Cu	Mn	Fe	Si
Fe01	α-Fe	77.42	9.58	0.67	11.10	1.23
Fe05	α-Fe	75.28	9.62	3.98	10.13	1.41
	β-Fe	67.83	27.30	0.60	4.27	...
Fe07	α-Fe	73.91	8.86	3.19	13.41	0.61
	β-Fe	67.03	22.64	1.47	8.86	...
	Al_6(FeMn)	84.20	4.71	1.60	9.49	...
	Al_6(FeMn)	83.01	5.20	2.88	8.86	...
Fe10	Al_3(FeMn)	77.09	6.8	4.55	11.33	...
	β-Fe	73.87	19.87	1.20	5.06	...
	Al_6(FeMn)	83.75	4.98	2.15	9.13	...
Fe15	Al_3(FeMn)	72.44	7.2	5.38	14.98	...
	β-Fe	79.70	17.18	0.84	2.28	...

D. Effect of the Fe content on the tensile properties of Al–5.0Cu–0.6Mn alloys

Figure 8 compares the tensile properties of alloys with different Fe contents and different applied pressures. The tensile properties are significantly enhanced as the applied pressure was increased from 0 to 75 MPa, especially the elongation. The reason may be attributed to the refinement of α (Al), the decrease of porosities and the evolution of Fe-rich intermetallics resulted by the applied pressures.[19] The elongation of the alloys gradually decreases with the Fe content, with a maximum of the ultimate mechanical strength and the yield strength observed for the alloys containing 0.5% Fe.

IV. DISCUSSION

A. Formation of Fe-rich intermetallics in gravity die cast alloys with different Fe contents

Combining the results of the systematic metallographic observations and DSC investigations described above with the results published by Backerud et al.,[5] Mondolfo[21] Kamaga et al.,[12] and Liu et al.,[13–15] the possible solidification reactions, their sequence of occurrence and the peak dissolution temperature for gravity die cast

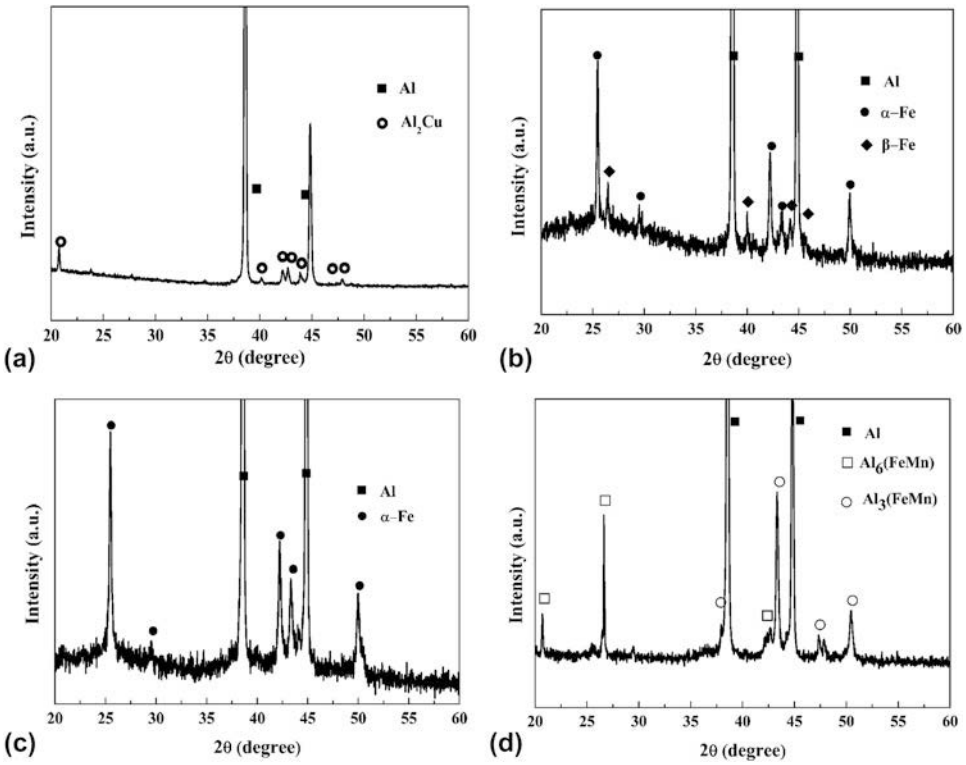

FIG. 2. XRD patterns of alloys: (a) 1.0% Fe, un-deep etched; (b) 0.5% Fe, deep etched; (c) 0.7% Fe, deep etched; (d) 1.0% Fe, deep etched.

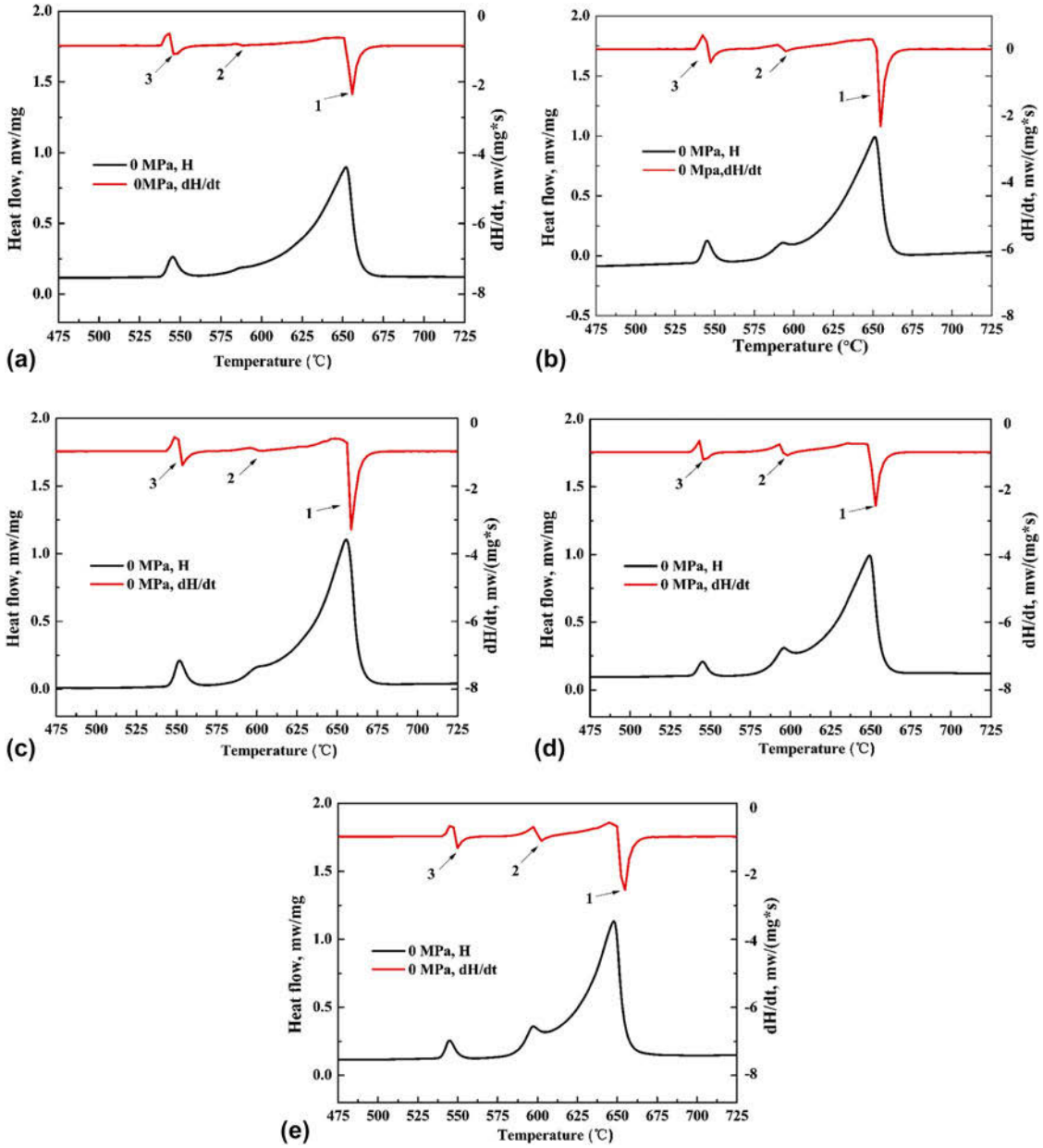

FIG. 3. DSC heating curves of the gravity die cast alloys with different Fe contents: (a) 0.1%; (b) 0.5%; (c) 0.7%; (d) 1.0%; (e) 1.5%.

Al–5.0Cu–0.6Mn alloys with different Fe contents are listed in Table III.

Al_3Fe and Al_6Fe are common Fe-rich intermetallics in AA1xxx (Al–Fe–Si) alloys. Backerud et al. found that the formation of aluminum dendrites begins at a temperature of 649–651 °C, and the $Al_6(FeMn)$ phase starts to form at 649 °C in A204 Al–Cu cast alloys.[5] According to Liu et al., the shape and position of the peaks attributed to $Al_3(FeMn)$ and $Al_6(FeMn)$ will resemble the Al dendrite peak in A206 Al–Cu alloys.[14] Therefore, only one peak is observed in this temperature range, indicating that the peaks for Al dendrite, $Al_3(FeMn)$, and $Al_6(FeMn)$ overlap in peak #1.

As shown in Table III, peak #2 indicates the formation of α-Fe, β-Fe, and $Al_6(FeMn)$. In alloys with a low Fe content (<1.0%), $Al_6(FeMn)$ takes part in the reaction associated with peak 2, resulting in the formation of the α-Fe and β-Fe phases, respectively [Figs. 4(b) and 1(d)].[22] Furthermore, the α-Fe partly transforms into β-Fe, as illustrated by Figs. 1(b) and 1(c). In alloys with a high Fe content (>1.0%), $Al_3(FeMn)$ takes part in the reaction associated with peak 2, resulting in the formation of the $Al_6(FeMn)$ and β-Fe phases, respectively [Figs. 4(h) and 1(e)].

Here, peak #3 is attributed to the main eutectic reaction because, in this study, this reaction is present in all alloys,

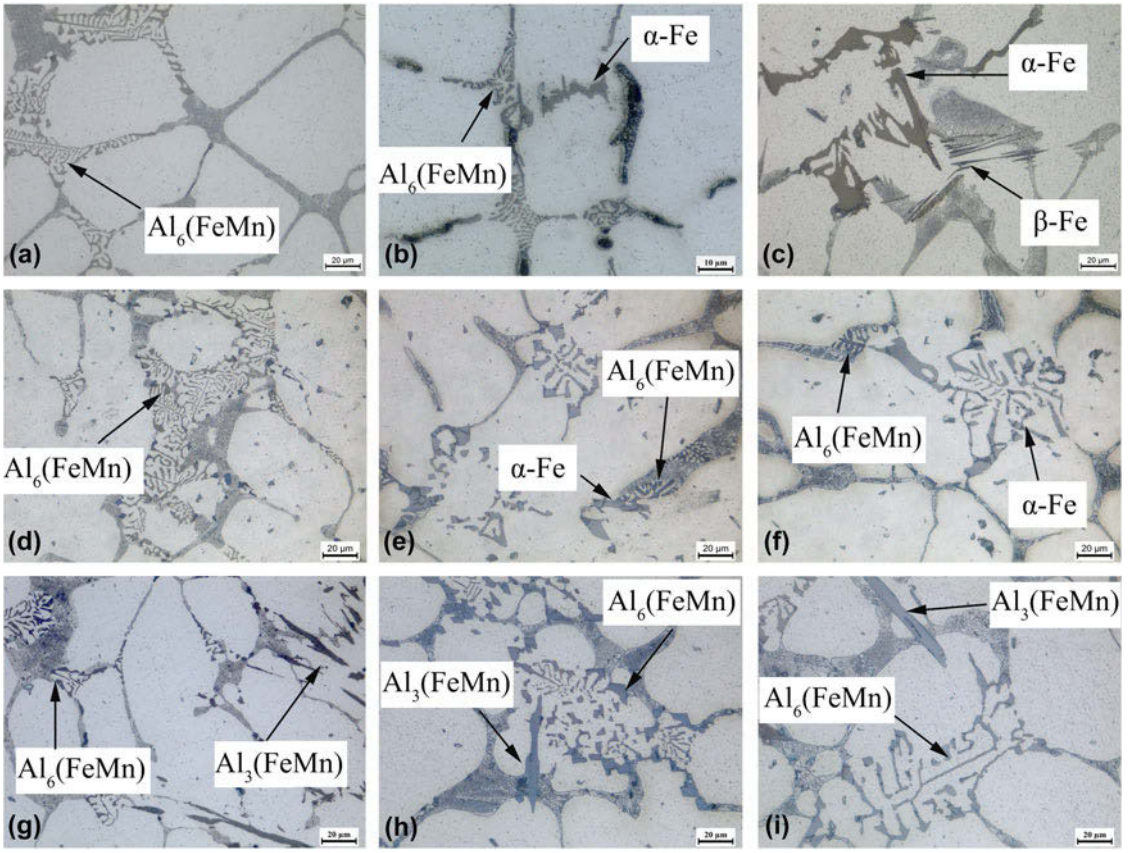

FIG. 4. Microstructures of alloys water quenching at different temperatures without applied pressure: (a) 0.5% Fe, 620 °C; (b) 0.5% Fe, 600 °C; (c) 0.5% Fe, 570 °C; (d) 0.7% Fe, 620 °C; (e) 0.7% Fe, 600 °C; (f) 0.7% Fe, 570 °C; (g) 1.0% Fe, 620 °C; (h) 1.0% Fe, 600 °C; (i) 1.0% Fe, 570 °C.

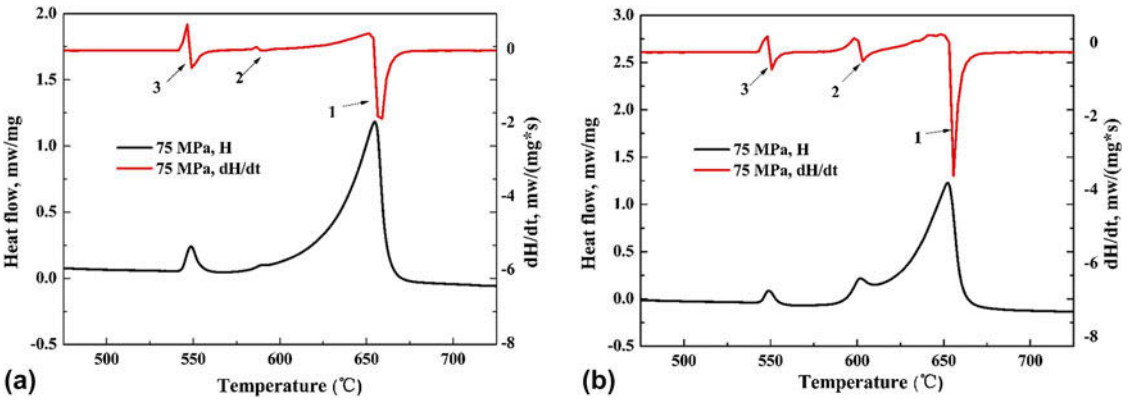

FIG. 5. DSC heating curves of the squeeze-cast alloys with different Fe contents: (a) 0.1%; (b) 1.5%.

independent of the Fe content. The formation of the β-Fe phase during the main eutectic reaction depends on the Fe content.

B. Effect of the applied pressure on the formation of Fe-rich intermetallics in Al–5.0Cu–0.6Mn alloys

The applied pressure reduces the amount of needle-like β-Fe and Al_3(FeMn).[19] This phenomenon may be related to the selective promotion of Fe-rich intermetallics by a high cooling rate in squeeze-cast alloys. As already demonstrated earlier, higher cooling rates can be achieved during solidification in the squeeze-casting process.[23,24] Previous studies suggested that a high cooling rate promotes the formation of Al_6(FeMn) over the formation of Al_3(FeMn) in AA1xxx(Al–Fe–Si) alloys[25] and AA5182 alloys.[26] Furthermore, the Al–Al_6Fe eutectic phase grows

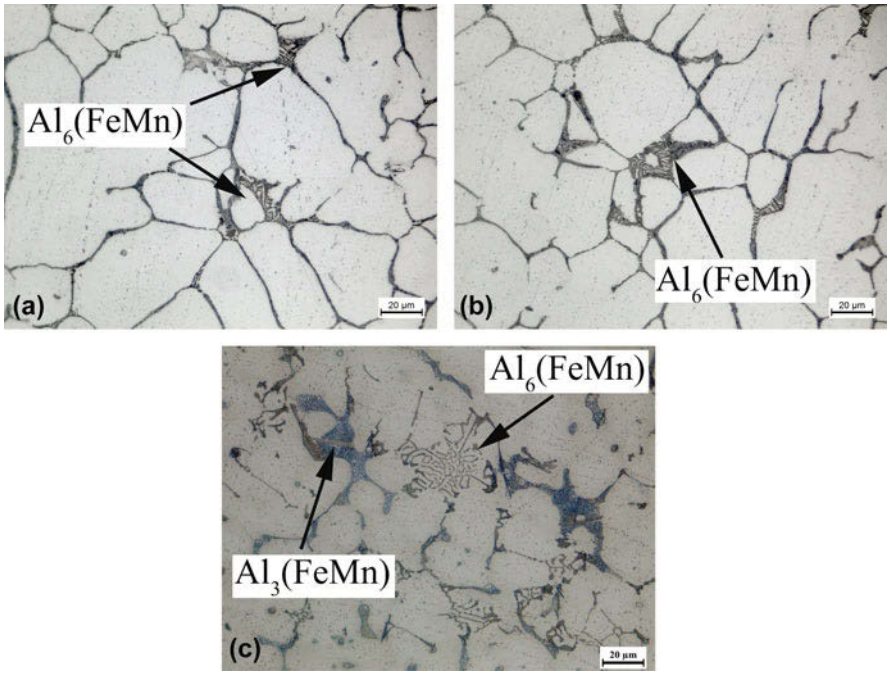

FIG. 6. Microstructures of water quenching samples at 620° C with the applied pressure of 75 MPa: (a) 0.5%; (b) 0.7%; (c) 1.0%.

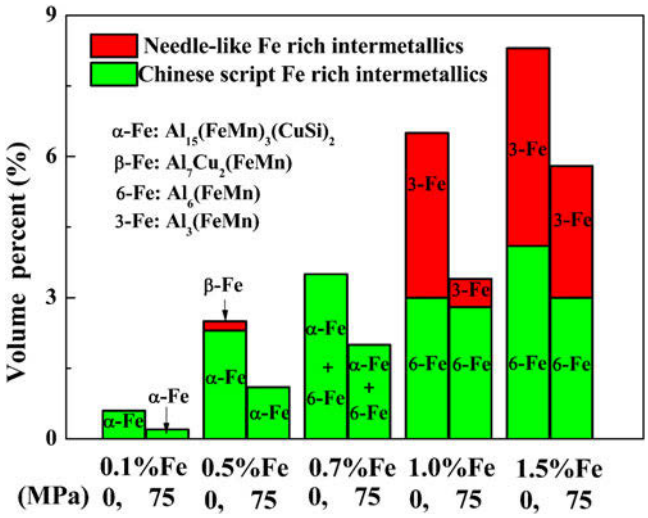

FIG. 7. Volume percent of Fe-rich intermetallics of alloys with different Fe contents and applied pressures.

at a higher temperature than the Al–Al_3Fe eutectic phase in the Al–Fe alloy at high solidification velocities.[27] Similarly, the applied pressure will promote the formation of Al_6(FeMn) and prevent the precipitation of Al_3(FeMn) during squeeze casting at high cooling rates (cp. Fig. 6).

The second reason is related to the crystal structure of the Fe-rich intermetallics. The α-Fe phase has a cubic structure, and nucleates and grows more easily and more quickly than the tetragonal β-Fe phase, whereas the β-Fe and Al_3(FeMn) phases exhibit a thin needle-like morphology, which indicates the rate of transformation of these phases is essentially governed by the mobility of the large facets.[12] That is to say, the growth rate of Fe-rich intermetallics is governed by the mobility of solute, especially the Fe, because the low solute normalized growth restriction factor of Fe in aluminum alloys.[28]

The connection of solute normalized growth restriction factor and the applied pressure can be expressed by the Eq. (1) (Ref. 29):

$$D = \frac{RT}{\delta\eta_0 \exp\left(\frac{PV_0}{RT}\right)} \quad , \tag{1}$$

where D is the solute normalized growth restriction factor; δ is the length of atomic free path; η_0 is the viscosity, V_0 is the original volume of liquid phase; therefore, the ratio between the solute normalized growth restriction factor of the squeeze casting (applied pressure of 75 MPa) and gravity die casting (applied pressure of 0 MPa) can be expressed as the Eq. (2):

$$\frac{D_P}{D_0} = \exp\left[\frac{(P_0 - P) \times V_0}{RT}\right] = \exp\left[\frac{\left(1.01 \times 10^5 - 7.5 \times 10^7\right) \times V_0}{RT}\right] \quad . \tag{2}$$

From the Eq. (2), we can find that the solute normalized growth restriction factor will decrease with increasing the applied pressure. As a result, the thin needle-like β-Fe will form difficulty for the low diffusion and gather

ability of Fe in squeeze-casting alloys. Besides, the "early" formed α-Fe consumes the Fe, and the amount of free Fe available for β-Fe is reduced. Therefore, compared to the β-Fe and Al_3(FeMn) phases, α-Fe and Al_6(FeMn) can be formed more easily at high cooling rates. Figure 9 shows the DSC heating curves and their first differentiations obtained for the 0.6Mn–0.1Fe alloy for different applied pressures. The peak temperature of peak #2 in the Fe01 alloy increases with the applied pressure (peak #2 is related to the formation of α-Fe). A high applied pressure increases the precipitation temperature of α-Fe. Therefore, the DSC heating curves further confirm that a high applied pressure promotes the formation of α-Fe.

In addition, high pressures decrease the critical radius for nucleation and decreases the interfacial free energy of crystal interface.[30] That is to say, the applied pressure will increase the nucleation of Fe-rich intermetallics. Therefore, a large amounts and small size of Fe-rich intermetallics will be obtained in squeeze-cast alloys.

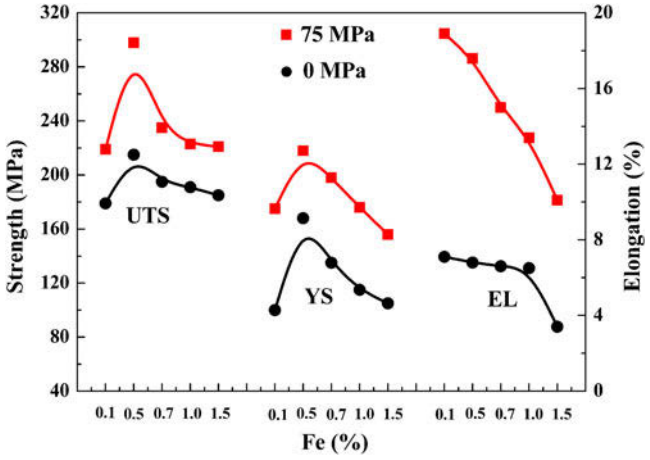

FIG. 8. Tensile properties of the alloys with different Fe contents and applied pressures.

TABLE III. Possible solidification reactions in gravity die cast Al–5.0Cu–0.6Mn alloy with different Fe contents.

NO	Reactions	Temperature (°C)	Alloys
1	(a) L → α (Al)	649–653	Fe01–Fe15
	(b) L → α (Al) + Al_3(FeMn)	...	Fe10–Fe15
	(c) L → α (Al) + Al_6(FeMn)	...	Fe01–Fe15
2	(a) L + Al_6(FeMn) → α-Fe	589–597	Fe01–Fe05
	(b) L + α-Fe → β-Fe	...	Fe05–Fe07
	(c) L + Al_3(FeMn) → α (Al) + β-Fe	...	Fe10–Fe15
	(d) L + Al_3(FeMn) → α (Al) + Al_6(FeMn)	...	Fe10–Fe15
	(e) L + Al_6(FeMn) → α (Al) + β-Fe	...	Fe05–Fe15
3	L → α (Al) + Al_2Cu + β-Fe	546–547	Fe01–Fe15

C. Effect of the Fe content on the tensile properties of Al–5.0Cu–0.6Mn alloys

As indicated by Fig. 8, the alloy elongation gradually decreases with the Fe content, and the maximum value for both the ultimate mechanical strength and the yield strength was found for the alloys with 0.5 wt% Fe. This is attributed to the morphology and amount of Fe-rich intermetallics. To disclose the morphologies of the Fe-rich intermetallics, some selected specimens were deep-etched. Representative SEM micrographs revealing the typical three dimensional morphologies of the Fe-rich intermetallics are shown in Fig. 10. The coarse β-Fe phases precipitate with a coarse plate-shape morphology as shown in Fig. 10(a). As shown in Fig. 10(b), the α-Fe phase exhibits a typical dendrite structure. Some primary branches with different sizes grow from a center and some secondary branches can grow directly from the sides of the large primary axes.

The morphology of Al_3(FeMn) in the deep-etched samples exhibits twinning characteristics, i.e., some branches in different growth directions [Fig. 10(c)], whereas Al_6(FeMn) shows a skeletal structure [Fig. 10(d)]. Therefore,

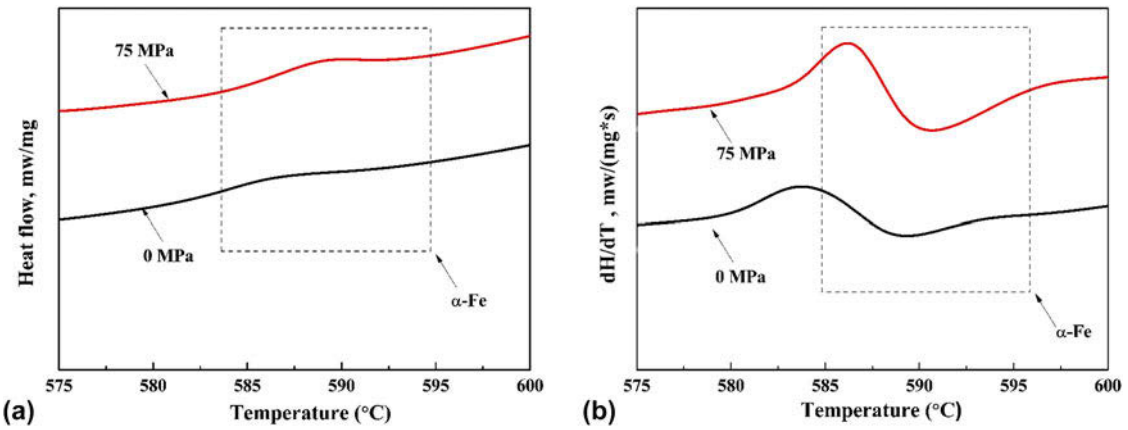

FIG. 9. (a) DSC heating curves and (b) their first differentiations for 0.6Mn–0.1Fe alloy at various applied pressures.

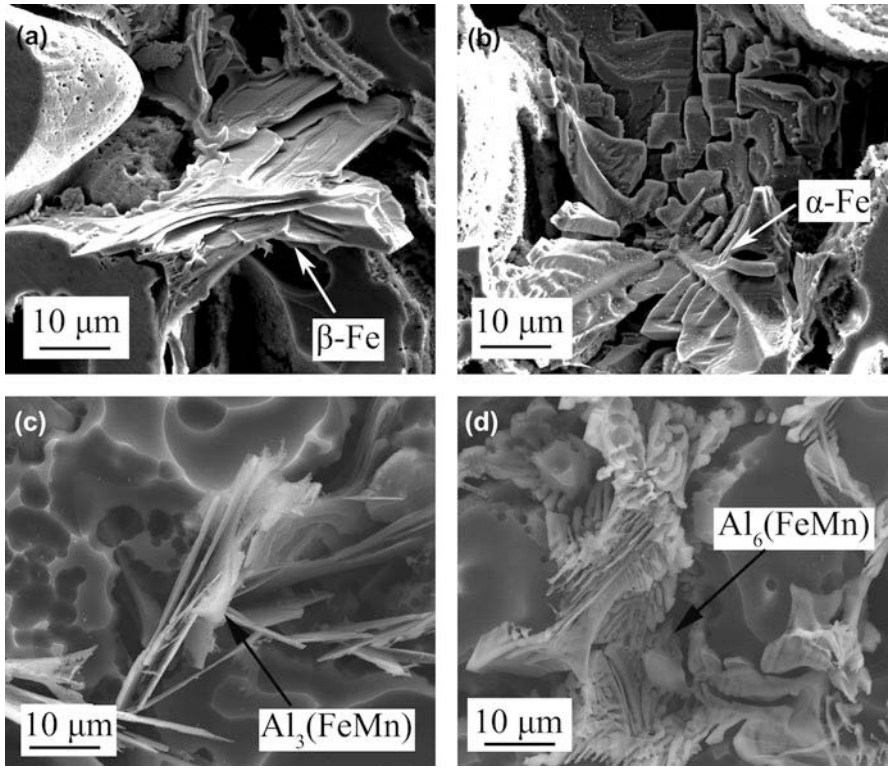

FIG. 10. SEM images of the Fe-rich intermetallics in deep etched samples: (a) 0.1%; (b) 0.5%; (c) 0.7%; (d) 1.0%.

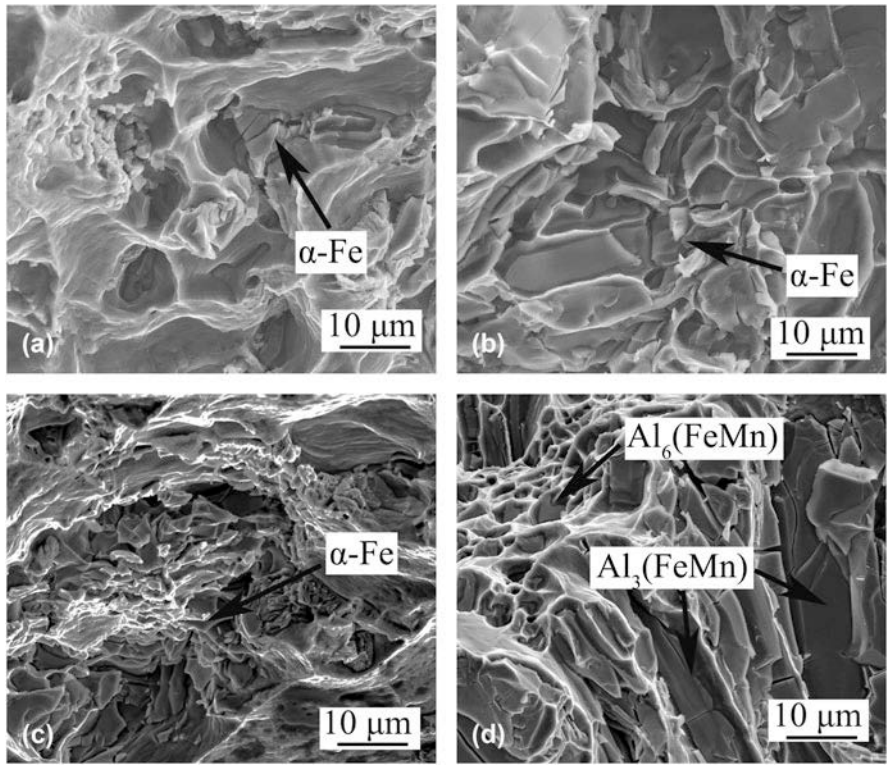

FIG. 11. Morphologies of Fe-rich intermetallics in fracture surfaces of alloys: (a) 0.1%; (b) 0.5%; (c) 0.7%; (d) 1.0%.

the plate-shaped β-Fe and Al_3(FeMn) can easily become crack initiation sites, while the compact α-Fe and Al_6(FeMn) are less harmful to the mechanical properties.[16] Figure 11 reveals the morphology of Fe-rich intermetallics on the fracture surfaces of the alloys. It can be observed that the α-Fe and Al_6(FeMn) phases usually exist inside ductile dimples, which suggests that they are less harmful than the plate-shaped Al_3(FeMn).

As it is shown in Fig. 7, the main Fe-rich intermetallic phase is α-Fe, with only 0.2% volume percent β-Fe existing in the Fe05 alloy. A small amount of α-Fe is beneficial by improving the alloy strength through second phase hardening in alloys with a low Fe content. In contrast, the increased concentration of Fe-rich intermetallics, especially the needle-like Al_3(FeMn) in alloys with a high Fe content results in the deterioration of the tensile properties. Therefore, a maximum value for both the ultimate mechanical strength and the yield strength was found for the alloys with 0.5 wt% Fe.

V. CONCLUSIONS

The formation of Fe-rich intermetallics and their effect on the tensile properties of squeeze-cast Al–5.0Cu–0.6Mn alloys with different Fe contents have been investigated. The conclusions are as follows:

(1) The main Fe-rich intermetallics observed are α-Fe [$Al_{15}(FeMn)_3(CuSi)_2$] and needle-like β-Fe [Al_7Cu_2(FeMn)] in Al–5.0Cu–0.6Mn alloys with a low Fe content, and they change into Al_6(FeMn) and needle-like Al_3(FeMn) in alloys with a high Fe content.

(2) According to the microstructure investigations performed on water quenched specimens, the primary Fe-rich intermetallics which formed from the Al alloy melt were Al_6(FeMn) and Al_3(FeMn). Al_6(FeMn) preferably precipitates in alloys with a low Fe content (below 0.7%), partly or completely changing into β-Fe or α-Fe, respectively, after solidification. Al_3(FeMn) preferably forms in alloys with a high Fe content (above 1.0%), partly or completely changing into β-Fe or Al_6(FeMn), respectively, after solidification.

(3) The applied pressure promotes the formation of Fe-rich intermetallic α-Fe or Al_6(FeMn) phases and prevents the precipitation of needle-like β-Fe or Al_3(FeMn). The formation temperature of α-Fe increases with the applied pressure.

(4) The elongation of the alloys gradually decreases with the Fe content. A maximum value for both the ultimate mechanical strength and the yield strength was found for the alloys with 0.5 wt% Fe. The reason is that the α-Fe and Al_6(FeMn) phases are beneficial for the strength but are harmful to the toughness of the alloys. The tensile properties of the alloys with different Fe contents significantly increased as the applied pressure was increased from 0 to 75 MPa, especially the elongation.

ACKNOWLEDGMENTS

The financial support from the Natural Science Foundation of China (51374110), Specialized Research Fund for Doctoral Program of Higher Education (20120172110045) and Research Found for Doctoral Program of Gui Zhou University (201440) is acknowledged.

REFERENCES

1. X. Cao and J. Campbell: Morphology of β-Al_5FeSi phase in Al-Si cast alloys. *Mater. Trans.* **47**(5), 1303 (2006).
2. X. Cao and J. Campbell: The solidification characteristics of Fe-rich intermetallics in Al-11.5 Si-0.4 Mg cast alloys. *Metall. Mater. Trans. A* **35**(5), 1427 (2004).
3. X. Cao and J. Campbell: The nucleation of Fe-rich phases on oxide films in Al-11.5 Si-0.4 Mg cast alloys. *Metall. Mater. Trans. A* **34**(7), 1409 (2003).
4. J.Y. Hwang, H.W. Dotyb, and M.J. Kaufman: The effects of Mn additions on the microstructure and mechanical properties of Al-Si-Cu casting alloys. *Mater. Sci. Eng., A* **488**, 496 (2008).
5. L. Backerud, G. Chai, and J. Tamminen: *Solidification Characteristics of Aluminum Alloys*, Vol. **2** (AFS, Foundry Alloys, Oslo, Norway, 1990).
6. M.A. Talamantes-Silva, A. Rodriguez, J. Talamantes-Silva, S. Valtierra, and R. Colas: Characterization of an Al-Cu cast alloy. *Mater. Charact.* **59**, 1434 (2008).
7. C.J. Tseng, S.L. Lee, T.F. Wu, and J.C. Lin: Effects of Fe content on microstructure and mechanical properties of A206 alloy. *Mater. Trans. Jim* **41**(6), 708 (2000).
8. C.J. Tseng, S.L. Lee, T.F. Wu, and J.C. Lin: Effects of manganese on microstructure and mechanical properties of A206 alloys containing iron. *J. Mater. Res.* **17**(9), 2243 (2002).
9. K. Liu, X. Cao, and X.G. Chen: Solidification of iron-rich intermetallic phases in Al-4.5Cu-0.3Fe cast Alloy. *Metall. Mater. Trans. A* **42**(7), 2004 (2011).
10. K. Liu, X. Cao, and X.G. Chen: Effect of Mn, Si, and cooling rate on the formation of iron-rich intermetallics in 206 Al-Cu cast alloys. *Metall. Mater. Trans. B* **43**(5), 1231 (2012).
11. K.H. Kamga, D. Larouche, M. Bournane, and A. Rahem: Mechanical properties of aluminium-copper B206 alloys with iron and silicon additions. *Int. J. Cast Met. Res.* **25**(1), 15 (2012).
12. K.H. Kamga, D. Larouche, M. Bournane, and A. Rahem: Solidification of aluminum-copper B206 alloys with iron and silicon additions. *Metall. Mater. Trans. A* **41A**, 2844 (2010).
13. K. Liu, X. Cao, and X.G. Chen: A new iron-rich intermetallic-Al_mFe phase in Al-4.6Cu-0.5Fe cast alloy. *Metall. Mater. Trans. A* **43A**, 1097 (2012).
14. K. Liu, X. Cao, and X.G. Chen: Precipitation of iron-rich intermetallic phases in Al-4.6Cu-0.5Fe-0.5Mn cast alloy. *J. Mater. Sci.* **47**, 4290 (2012).
15. K. Liu, X. Cao, and X.G. Chen: Formation and phase selection of iron-rich intermetallics in Al-4.6Cu-0.5Fe cast alloys. *Metall. Mater. Trans. A* **44**(2), 682 (2013).
16. K. Liu, X. Cao, and X.G. Chen: Tensile properties of Al-Cu 206 cast alloys with various iron contents. *Metall. Mater. Trans. A* **45** (5), 2498 (2014).
17. J.X. Dong, P.A. Karnezis, G. Durrant, and B. Cantor: The effect of Sr and Fe additions on the microstructure and mechanical properties of a direct squeeze cast Al-7Si-0.3Mg alloy. *Metall. Mater. Trans. A* **30A**, 1341 (1999).
18. W.W. Zhang, B. Lin, J.L. Fan, D.T Zhang, and Y.Y. Li: Microstructures and mechanical properties of heat-treated

Al-5.0Cu-0.5Fe squeeze cast alloys with different Mn/Fe ratio. *Mater. Sci. Eng., A* **588**, 366 (2013).
19. B. Lin, W.W. Zhang, Z.H. Lou, D.T. Zhang, and Y.Y. Li: Comparative study on microstructures and mechanical properties of the heat-treated Al-5.0Cu-0.6Mn-xFe alloys prepared by gravity die casting and squeeze casting. *Mater. Des.* **59**, 10 (2014).
20. L. Sweet, S.M. Zhu, S.X. Gao, J.A. Taylor, and M.A. Easton: The effect of iron content on the iron-containing intermetallic phases in a Cast 6060 aluminum alloy. *Metall. Mater. Trans. A* **42A**, 1737 (2011).
21. L.F. Mondolfo: *Aluminum Alloys: Structure and Properties* (Butterworths, London, UK, 1976).
22. N.A. Belov, A.A. Aksenov, and D.G. Eskin: *Iron in Aluminium Alloys: Impurity and Alloying Element* (CRC Press, London, UK, 2002).
23. D.Y. Maeng, J.H. Lee, C.W. Won, S.S. Cho, and B.S. Chun: The effects of processing parameters on the microstructure and mechanical properties of modified B390 alloy in direct squeeze casting. *J. Mater. Process. Technol.* **105**, 196 (2000).
24. A. Maleki, A. Shafyei, and B. Niroumand: Effects of squeeze casting parameters on the microstructure of LM13 alloy. *J. Mater. Process. Technol.* **209**, 3790 (2009).
25. H. Westengen: Formation of intermetallic compounds during DC-casting of a commercial purity Al-Fe-Si. *Z. Metallkd.* **73**(6), 360 (1982).
26. Y.J. Li and L. Arnberg: Solidification structures and phase selection of iron-bearing eutectic particles in a DC-cast AA5182 alloy. *Acta. Mate.* **52**(9), 2673 (2004).
27. B. Dutta and M. Rettenmayr: Effect of cooling rate on the solidification behaviour of Al-Fe-Si alloys. *Mater. Sci. Eng., A* **283**(1), 218 (2000).
28. L. Arnberg, L. Backerud, and G. Chai: *Solidification Characteristics of Aluminum Alloys* (AFS Inc., Des Plaines, IL, 1996).
29. A.I. Batyshev: *Crystallization of Metals and Alloys under Pressure* (Cambridge International Science Publishers, London, UK, 2002).
30. J.J. Sobczak, L. Drenchev, and R. Asthana: Effect of pressure on solidification of metallic materials. *Int. J. Cast Met. Res.* **25**(1), 1 (2012).